

Modeling First-Pass Ethanol Metabolism in the Human Hepatic Lobule

Matthew Cai

Andrew Bernardo

Molly Allen

BENG221

November 16, 2012

Table of Contents

Background and Introduction	3
Model and Assumptions.	4
Solution of Complete Model (with Convection and Consumption)	5
Solution of Simplified Model (without Convection BUT with Consumption)	8
Solution of Simplified Model (without Convection and Consumption)	9
Conclusions	12
References	13
Appendix A: Analytical Solution	13
Appendix B: MATLAB Code for Finite Differences.	17

Introduction and Background

The primary site of ethanol metabolism is in the liver. When ethanol is ingested, it is rapidly absorbed into the bloodstream through capillaries in the stomach and small intestines. Veins carry the ethanol to the liver through which it is perfused and metabolized. Ethanol is converted into acetaldehyde via alcohol dehydrogenase, catalase, and CYP2E1 enzymes, and from acetaldehyde into acetate via aldehyde dehydrogenases which is then removed from the body.^{1,2}

The amount of alcohol in an individual's system is measured by the percent by volume of ethanol in the blood, called the blood alcohol concentration (BAC). The amount of ethanol in the blood for a given quantity of ingested alcohol varies widely from person to person and depends on an individual's absorption, distribution, metabolism, and excretion rates. These rates in turn are influenced by factors such as age, sex, genetics, fasting or fed state, type of alcohol, rate and frequency of alcohol consumption, and even time of day. However, a session of moderate alcohol consumption will typically result in a BAC within the range of 0.046-0.092, or about 10-20 mM. This ethanol is circulated throughout the body, eventually passing through the liver via the portal veins.¹

The liver is made up of 1-1.5 million functional units called hepatic lobules. In cross-section, hepatic lobules are multicellular structures of hexagonal shape centered about a central vein and bordered at six corners by portal triads (see Figure 1). Each lobule is composed of the metabolically active liver cells called hepatocytes between which run endothelial cell-lined channels called sinusoids. Blood from the portal veins and hepatic arteries within the portal triads perfuse from the outer edge of each lobule through the sinusoids, passing by the metabolically active hepatocytes, and drain into the central vein.²

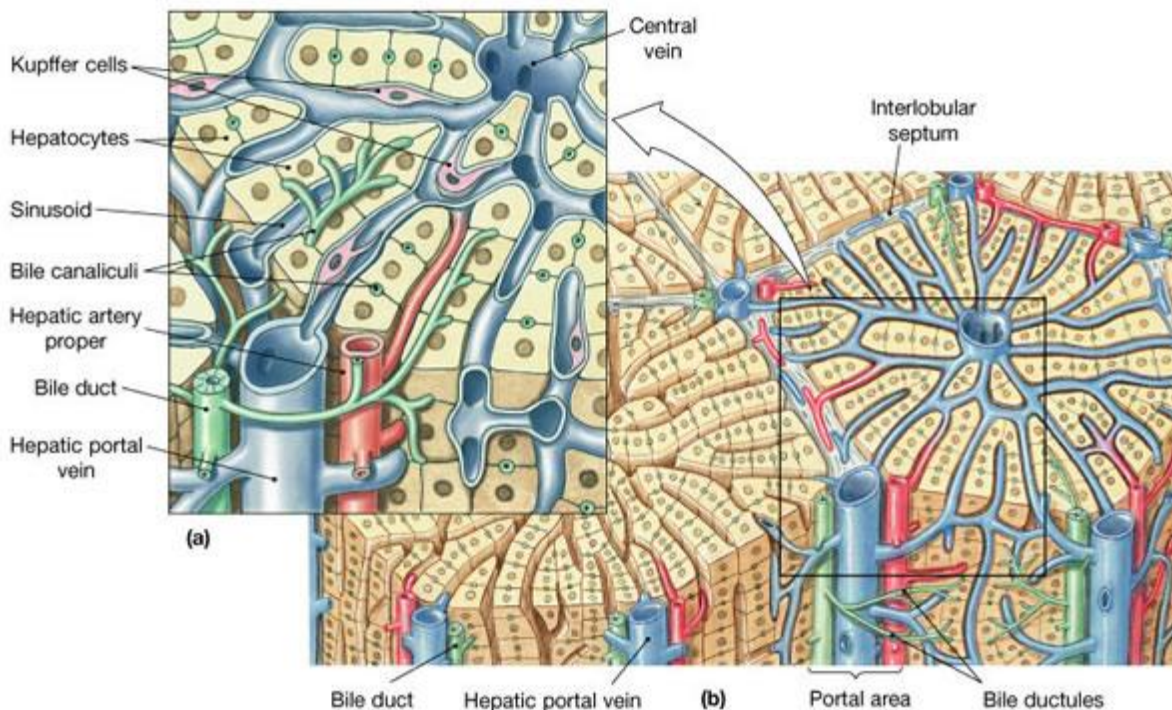


Figure 1 Schematic of the hepatic lobule. (Copyright © 2004 Pearson Education)

Model and Assumptions

To study the alcohol concentration within the hepatic lobule, we approximated its geometry as a hollow cylinder (Figure 2a). The inner radius R_1 represents the radius of the central vein which is $100\ \mu\text{m}$. The outer radius R_2 represents the radius of the entire lobule. With an average lobule thickness from the central to the portal veins of about 15 hepatocytes, each $50\ \mu\text{m}$ in diameter, giving a cylinder thickness of $750\ \mu\text{m}$. Factoring in the radius of the central vein, this gives a total lobule radius R_2 of $850\ \mu\text{m}$.³

With this cylindrical geometry, we simplified the ethanol-rich blood entering the lobule from each of the six portal triads by setting a constant value ethanol concentration of $20\ \text{mM}$ at the boundary R_2 . Although in the body ethanol concentration is not constant over time, we will only be looking at the model in a time period of a few minutes, thus making this a reasonable approximation. Inside, at the edge of the central vein (boundary R_1), we set the alcohol concentration to be $0\ \text{mM}$, assuming that the central vein quickly carries away any un-metabolized ethanol maintaining an ethanol free boundary. Additionally, we set the initial concentration of ethanol within the hepatic lobule at $0\ \text{mM}$ throughout to simulate an ethanol-free initial condition.

Furthermore, we assumed radial symmetry (i.e. the same ethanol concentration profile for all θ) within the lobule, and that the blood alcohol concentration along the lobule's central axis (in the z -direction) is uniform. Therefore, the concentration of ethanol in the lobule depends only on the radius and time, reducing our model to a 2D polar coordinate approximation (Figure 2b).

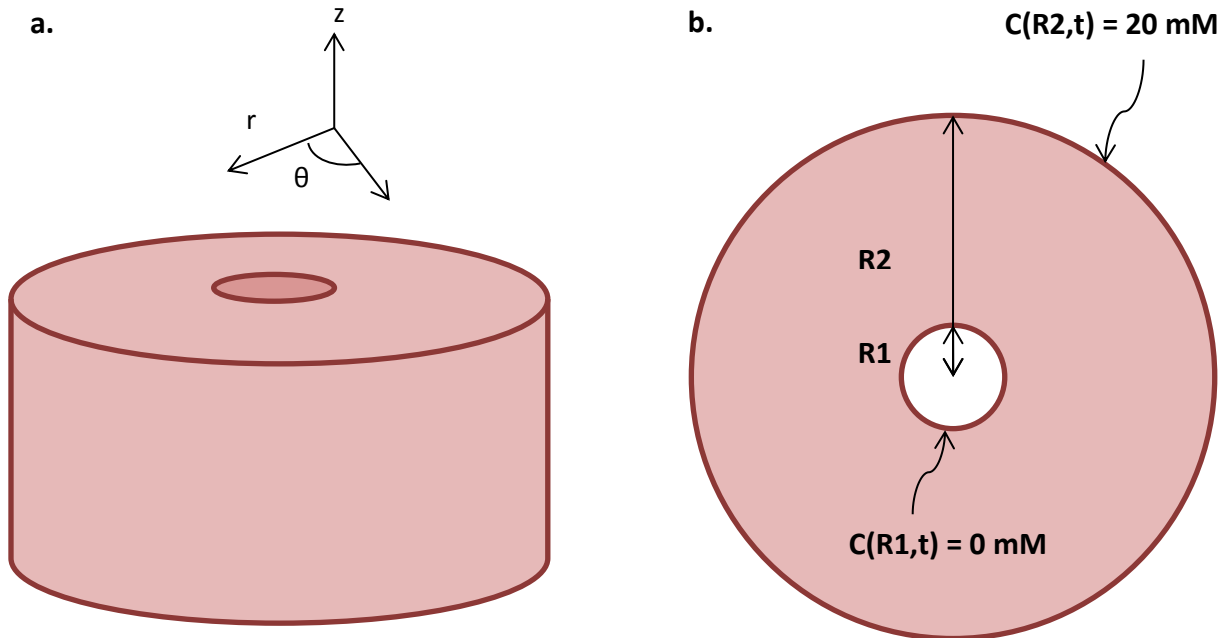


Figure 2: Geometry of the mathematical model of the hepatic lobule. **a.** 3D hollow cylinder approximation of a single hepatic lobule. **b.** Simplified 2D model of hepatic lobule including value boundary conditions for ethanol concentration assuming radial symmetry and uniform concentration in the z -direction.

Because blood is continuously flowing into the lobule (from R_2 to R_1) through sinusoids and diffuses readily across tissues, the concentration of ethanol will depend both on convection and diffusion. Convection was approximated by assuming a constant blood velocity of 0.21 mm/s, which is the average velocity previously measured in rats by tracking erythrocyte flow through the sinusoids.⁴ Although radial convection is proportional to $1/r$, we chose to make it constant for simplicity. Due to ethanol molecules' rapid diffusion through tissues, the diffusivity of ethanol was approximated to be that of ethanol in water: $1.23 \times 10^{-9} \text{ m}^2/\text{s}$.⁵

To account for the actual metabolism of ethanol by the hepatocytes in the lobule, we introduced a concentration-dependent consumption rate modeled with Michaelis-Menton kinetics. While the liver employs a variety of different enzymes in ethanol metabolism, we chose to focus on the most abundant liver-specific alcohol dehydrogenase isozyme ADH1A, which has a Michaelis constant K_m of 4 mM and a maximum reaction velocity V_{max} of 0.5 mM/min.¹ The enzyme is assumed to be distributed evenly throughout the hepatic lobule, though it is actually located within the cytosol of the hepatocytes.¹

The concentration of ethanol within the hepatic lobule can be described by the conservation relations equation for dilute solutions⁶ as follows:

$$\frac{\partial C}{\partial t} + \overbrace{v_r \frac{\partial C}{\partial r}}^{\text{Convection}} = D \overbrace{\left(\frac{1}{r} \frac{\partial}{\partial r} \left(r \frac{\partial C}{\partial r} \right) \right)}^{\text{Diffusion}} - \overbrace{\frac{V_m C}{K_m + C}}^{\text{Consumption}}$$

where C is the concentration of ethanol, t is time, r is the radius, v_r is the blood velocity through the sinusoids, D is the diffusivity of ethanol, V_m is the V_{max} or maximum reaction rate of ADH1A, and K_m is the Michaelis constant for ADH1A. Note that the terms in the equation describing concentration changes in the θ and z directions equal zero since the concentration C is assumed to depend only on radius r and time t . Table 1 below summarizes our model's parameters, initial conditions, and boundary conditions.

Parameter	Description	Value
R_1	Radius of central vein	100 μm
R_2	Radius of hepatic lobule	850 μm
$C(R_1, t)$	Zero value ethanol concentration BC at R_1	0 mM
$C(R_2, t)$	Value ethanol concentration BC at R_2	20 mM
$C(r, 0)$	Zero value ethanol concentration IC	0 mM
D	Diffusivity of ethanol through water (STP)	$1.23 \times 10^{-9} \text{ m}^2/\text{s}$
K_m	Michaelis constant of ADH1	4 mM
V_{max}	Maximum reaction velocity of ADH1	0.5 mM/s
v_r	Inward radial convective flow velocity	0.21 mm/s

Table 1: Summary of model parameters, initial conditions, and boundary conditions.

Solution of Complete Model (with Convection with Consumption)

$$\frac{\partial C}{\partial t} + v_r \frac{\partial C}{\partial r} = D \left(\frac{1}{r} \frac{\partial}{\partial r} \left(r \frac{\partial C}{\partial r} \right) \right) - \frac{V_m C}{K_m + C}$$

Because of the complexity of the partial differential equation with a nonlinear consumption term and the additional convection term, we could only find the solution using numerical methods. We chose to use finite differences⁸ because the PDEPE function in MATLAB⁷ cannot be used to solve nonlinear partial differential equations. The finite differences code can be found in Appendix B.

When using the physiological average velocity of 0.21 mm/s, the concentration in the sinusoid quickly reached close to the maximum concentration set at the outer boundary (Figure 3). The only factors preventing the entire ethanol concentration profile from being a uniform 20 mM is the zero-value inner boundary condition at R_1 as well as the consumption term. However, it is obvious in this case that the contribution from convection is much more significant in our model.

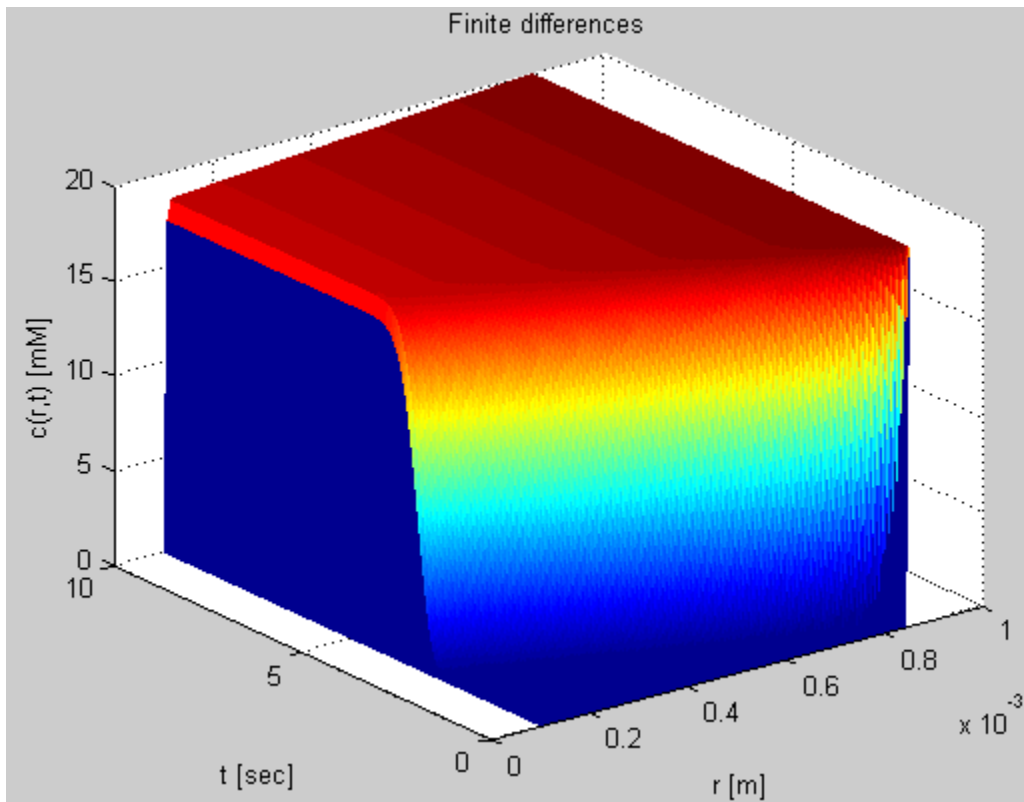


Figure 3. Numerical Solution of Complete Equation (Convection $v_r = -2.1 \times 10^{-4}$ m/s)

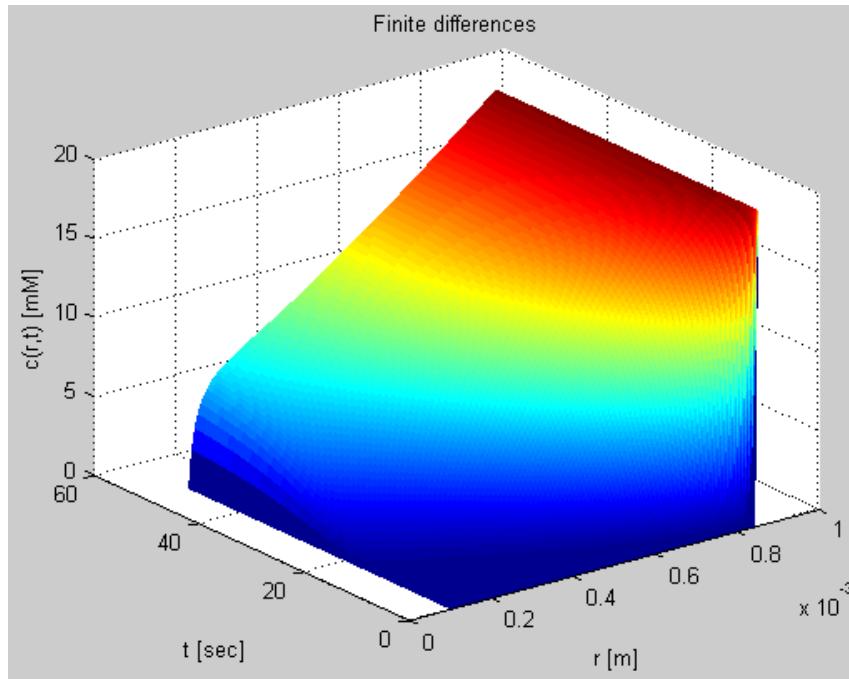


Figure 4. Numerical Solution of Complete Equation (Convection $v_r = -1.7 \times 10^{-6}$ m/s)

In order to better visualize the added effect of convection without it dominating the other terms in our partial differential equation, we decreased the flow rate and again plotted the numerical solution (Figure 4). Note that this eliminates the dominating 20 mM plateau region in Figure 3. By comparing steady state solutions with the solution to the equation without convection or consumption, it is apparent that convection increases the concentration near the inner radius R_1 because the flow is pushing the higher concentration on the outside radius R_2 towards the central vein (Figure 5).

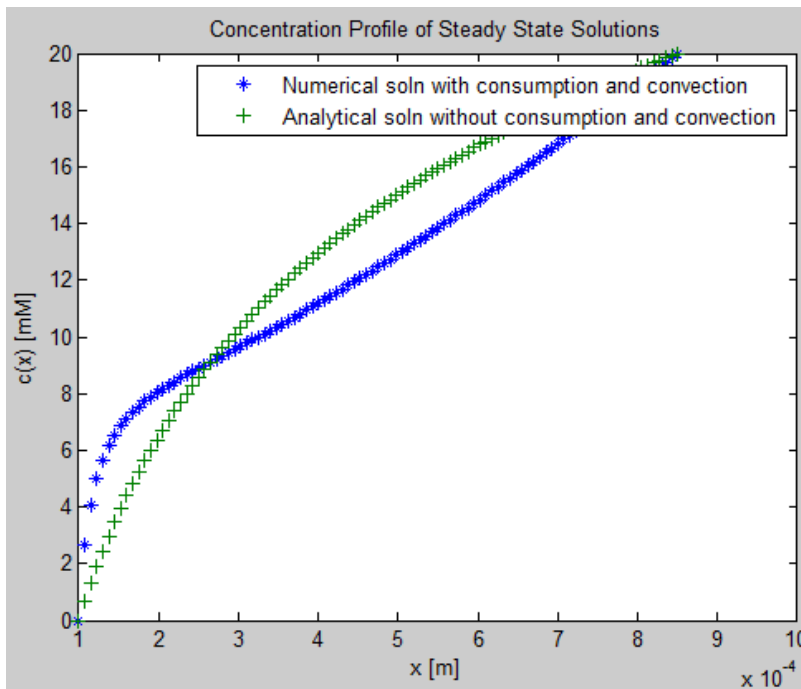


Figure 5. Comparing Steady State of Complete Model (with Convection with Consumption) shown in blue vs. Simplified Model (without Convection without Consumption) shown in green.

Solution of Simplified model (without Convection BUT with Consumption)

Disregarding our convection term, our partial differential equation reduces to:

$$\frac{\partial C}{\partial t} = D \left(\frac{1}{r} \frac{\partial}{\partial r} \left(r \frac{\partial C}{\partial r} \right) \right) - \frac{V_m C}{K_m + C}$$

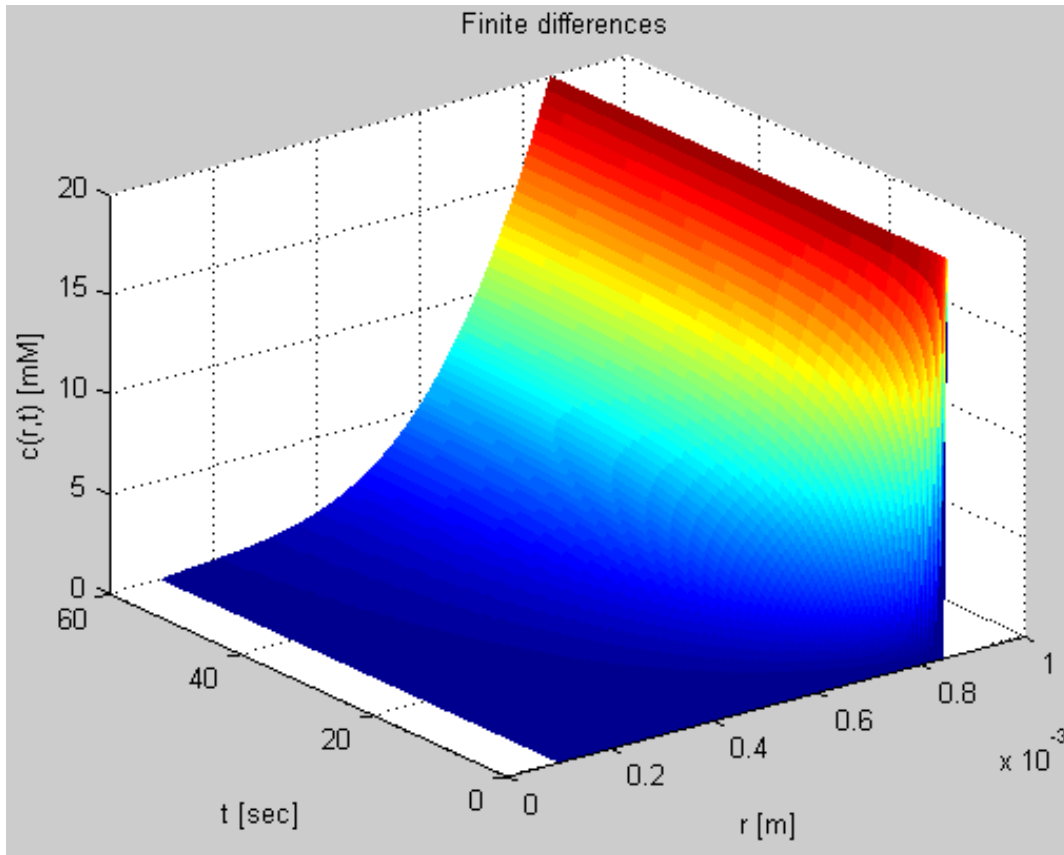


Figure 6: Numerical Solution of Simplified Model (without Convection BUT with Consumption)

To isolate the effect of consumption, we also found the numerical solution to the PDE without the convection term. By comparing it with the same steady state without convection or consumption, we can see the effect of consumption in Figure 7. The difference between the solutions is greatest near the outer boundary because that is where the concentration is highest. Because Michaelis-Menten enzyme kinetics dictate that the catalytic rate is higher at higher substrate concentrations, it is in this area where consumption has a greater effect.

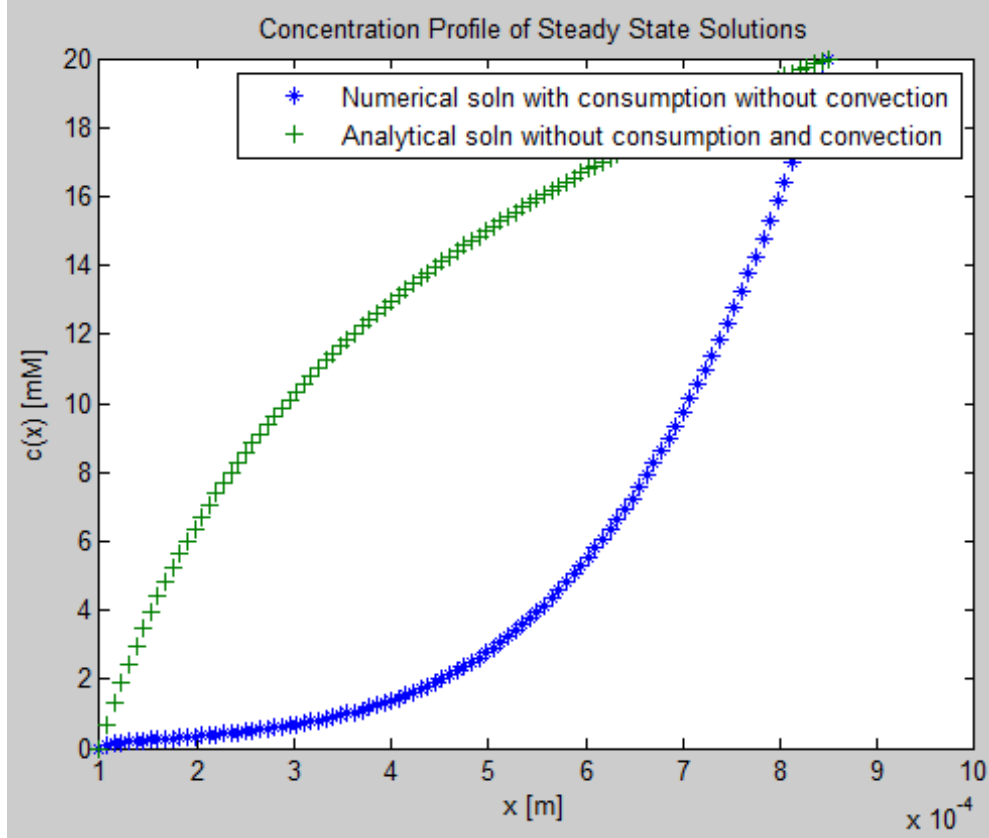


Figure 7: Comparing Effect of Consumption. Model without Consumption solved analytically and model with Consumption solved numerically. Neither has convection included.

Solution of Simplified Model (without Convection without Consumption)

In our most simplified case which disregards both convection and consumption:

$$PDE: \frac{\partial C}{\partial t} = D \left(\frac{1}{r} \frac{\partial}{\partial r} \left(r \frac{\partial C}{\partial r} \right) \right)$$

$$Solution: C(r, t) = -\pi \sum_{n=1}^{\infty} \frac{C(r = R_2) J_0(R_1 \alpha_n) J_0(R_2 \alpha_n) U_0(r \alpha_n)}{J_0^2(R_1 \alpha_n) - J_0^2(R_2 \alpha_n)} e^{-D \alpha_n^2 t} + \frac{C(r = R_2) \ln\left(\frac{r}{R_1}\right)}{\ln\left(\frac{R_2}{R_1}\right)}$$

By simplifying the model further to get rid of convection and consumption, we finally arrive at an equation we can solve analytically (see Appendix A). Because the equation does not have homogeneous boundary conditions we had to “extract the poison tooth”, resulting in a solution described by the sum of the steady state solution and the solution to the homogeneous boundary problem. To solve the homogeneous boundary problem, we used separation of variables that left us with a familiar time dependent exponential solution and a space dependent term the solution to which consisted of Bessel functions because of the cylindrical coordinates. Unfortunately because our cylinder boundaries do not include the axial center, the Bessel functions of the second kind do not blow up to infinity so we cannot disregard them in our solution. Therefore, our solution is in the form of a steady state solution added to an infinite series of two kinds of Bessel functions. We plotted the approximate analytical solution using 5

and 8 roots. As can be seen in Figures 8 and 9, an increasing number of terms results in a smoother, more accurate the solution, especially at early time points.

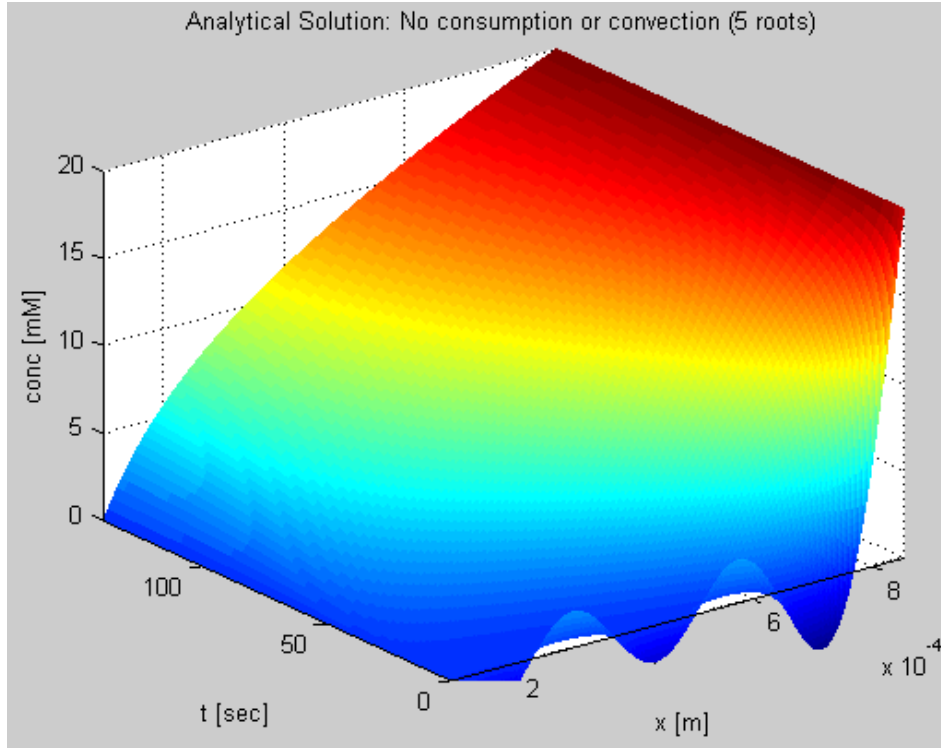


Figure 8: Analytical Solution of Simplified Model (without Convection without Consumption) approximated with first 5 roots

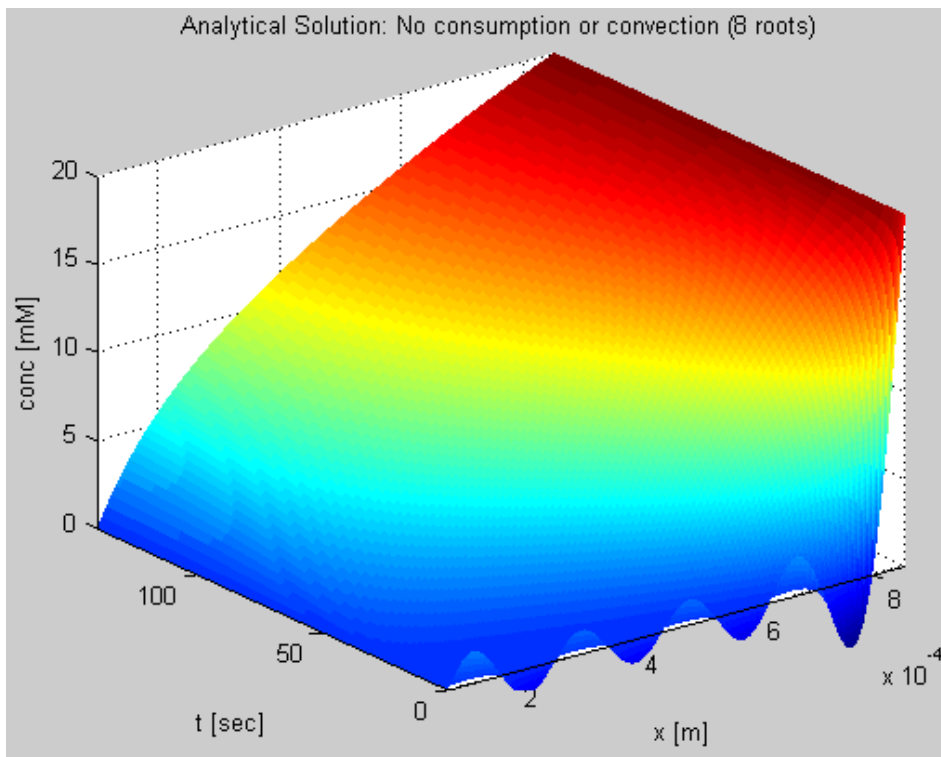


Figure 9: Analytical Solution of Simplified Model (without Convection without Consumption) approximated with first 8 roots

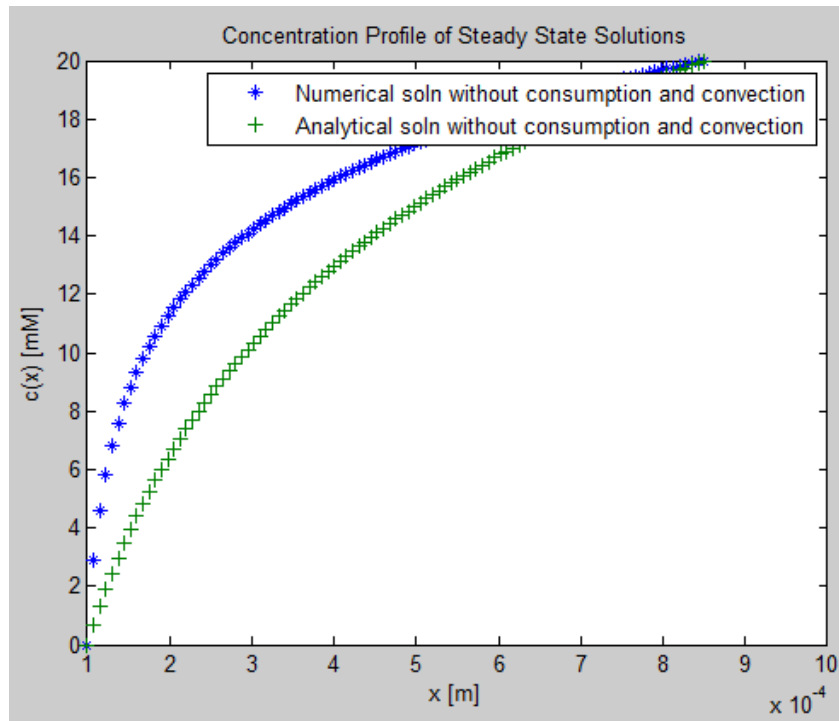


Figure 10: Comparing Steady States of Simplified Model solved with Numerical vs. Analytical methods

To verify our solutions, we plotted and compared the numerically and analytically derived steady states (Figures 10 & 11). While the match is not perfect, the general behavior is very close and distinct from the solutions when convection and consumption are added in. The difference in solutions can be accounted for by the approximating nature of the numerical methods and reminds us that numerically derived solutions are not exact. In the future, using smaller step sizes may help improve accuracy.

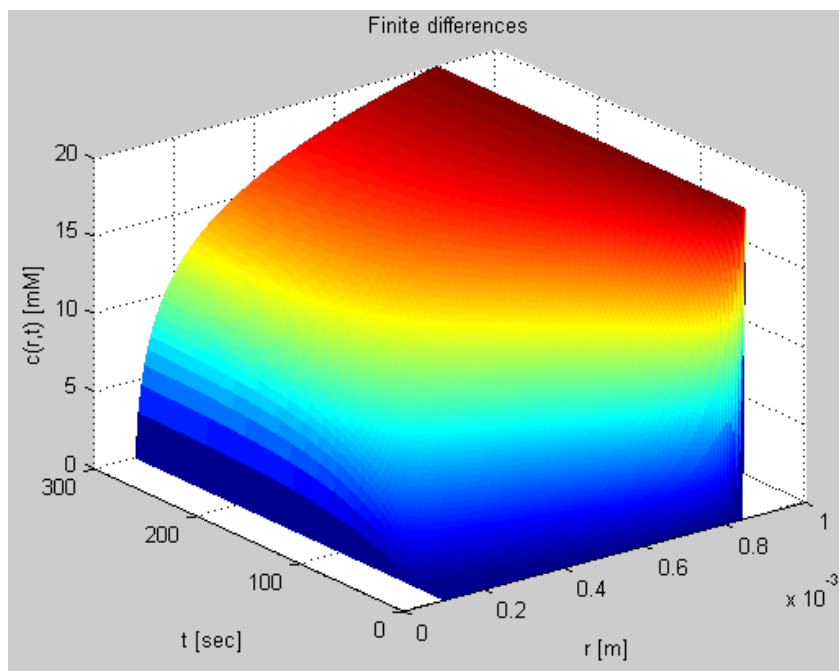


Figure 11: Numerical Solution of Simplified Model (without Convection without Consumption)

Conclusions

Our model sought to evaluate the ethanol concentration in the human hepatic lobule during first-pass ethanol metabolism. We were able to formulate and solve a partial differential equation with diffusive, convective, and consumptive terms using a number of assumptions for both the geometry and boundary conditions. Three different scenarios were modeled in order to observe how each term in our model affected the metabolism of ethanol in the hepatic lobule system.

Using a convective flow velocity of 0.21mm/s, we observed that the majority of the lobule remained at the maximum concentration of 20mM. This indicates that convection was the main force of ethanol movement, dominating both the diffusion and consumption factors in our overall equation. However, we know from the literature that distinct gradients of metabolites form within the hepatic lobule^{1,2}. This suggests that convection in our system represents an inaccurate representation of the natural physiology. This is not surprising considering the complex microarchitecture and non-uniform blood flow through the sinusoids.

In order to better observe the effects of both diffusion and consumption in our model, we greatly reduced the velocity of blood so that the convective term did not dominate the overall model. This allowed us to observe the concentration-dependent nature of our consumption term. By eliminating convection altogether, the Michaelis-Menten kinetics of ADH1A is even more apparent when compared to the analytical solution, which only considers diffusion. We find that the activity of ADH1A is highest at the outer boundary of R_2 due to the higher concentration of ethanol at this boundary.

In order to solve the partial differential equation analytically, the original partial differential equation was further simplified so that only diffusion in the r direction was considered, eliminating both convection and consumption from our problem. Using the “extracting the poison tooth” method, we were able to derive a solution that contained Bessel functions of both the first and second kind. Comparing our simplified analytical solution with our numerical method, we find that the solutions are not exactly the same. However, the two solutions do show similar behavior, both of which are distinctly different from the solutions that consider convection and/or consumption.

Due to the numerous assumptions that were made in solving the problem, the simplification of the hepatic lobule used to model the ethanol concentration during first-pass metabolism do not reflect real physiological conditions. In order to create a representative model of the complexity of metabolism in the hepatic lobule, more complex parameters and equations must be included. However, this may still lead to a numerical solution rather than the full analytical solution.

References

1. Zakhari S., "Overview: how is alcohol metabolized by the body?" *Alcohol Res Health* 2006; **29**: 245-257.
2. Vollmar B., & Menger M.D. "The hepatic microcirculation: mechanistic contributions and therapeutic targets in liver injury and repair." *Physiological Reviews* 2009; **89.4**: 1269-1339.
3. Wambaugh J., & Shah I. "Simulating Microdosimetry in a virtual hepatic lobule." *PLoS computational biology* 2010; **6.4**: e1000756.
4. Koo R., & Liang I. "Microvascular filling pattern in rat liver sinusoids during vagal stimulation." *J. Physiol.* 1979 (London), 295, pp. 191-199.
5. Hills E. E., et al. "Diffusion coefficients of ethanol in water at 298K: Linear free energy relationships." *Fluid Phase Equilibria* 2011; **45**: 303.
6. Truskey G.A., Yuan F., Katz D.F. *Transport phenomena in biological systems*. Vol. 82. Upper Saddle River, NJ: Pearson Prentic Hall, 2004.
7. MATLAB version R2012A. Natick, Massachusetts: The MathWorks Inc., 2012.
8. Olsen-Kettle, Louise. "Numerical solution of partial differential equations." *Earth Systems Science Computational Centre Publications* 2011.
http://espace.library.uq.edu.au/eserv/UQ:239427/Lectures_Book.pdf
9. Crank J. "The Mathematics of Diffusion: Diffusion in a Cylinder." 1979; Chapter 5.
10. Wolfram Research, Inc., Mathematica, Version 8.0, Champaign, IL 2011.
11. Carslaw, H.S., & Jaeger J.C. "Conduction of heat in solids." *Oxford: Clarendon Press* 1959; 2nd ed. 1: 205-208.

Appendix A – Analytical Solution

$$\frac{\partial C}{\partial t} = D \left(\frac{1}{r} \frac{\partial}{\partial r} \left(r \frac{\partial C}{\partial r} \right) \right) = D \left(\frac{1}{r} \left(r \frac{\partial^2 C}{\partial r^2} + \frac{\partial C}{\partial r} \right) \right)$$

Extraction of the "poison tooth"

$$C(r, t) = C_{ss} + C_{homogeneous}$$

Solving for the steady state solution:

$$\frac{\partial C}{\partial t} = D \left(\frac{1}{r} \frac{\partial}{\partial r} \left(r \frac{\partial C}{\partial r} \right) \right) = 0$$

Therefore,

$$\frac{\partial}{\partial r} \left(r \frac{\partial C}{\partial r} \right) = 0$$
$$r \frac{dC}{dr} = K_1, \quad \frac{dC}{dr} = \frac{1}{r} K_1$$

$$C(r) = K_1 \ln(r) + K_2$$

Plugging in general boundary conditions gives us

$$C_{ss} = \frac{C(r = R_1) \ln\left(\frac{R_2}{r}\right) + C(r = R_2) \ln\left(\frac{r}{R_1}\right)}{\ln\left(\frac{R_2}{R_1}\right)}$$

From this point on, $C = C_{homogeneous}$, with homogeneous boundary conditions

Separation of Variables

$$C = G(t)\Phi(r)$$

$$\frac{1}{D}\Phi(r)\frac{\partial G}{\partial t} = G(t)\frac{1}{r}\frac{\partial}{\partial r}\left(r\frac{\partial \Phi}{\partial r}\right)$$

$$\frac{1}{D}\frac{1}{G(t)}\frac{\partial G}{\partial t} = \frac{1}{\Phi(r)}\frac{1}{r}\frac{\partial}{\partial r}\left(r\frac{\partial \Phi}{\partial r}\right) = -\alpha^2$$

Time dependent portion

$$\frac{\partial G}{\partial t} = -\alpha^2 G(t)D$$

$$G(t) = e^{-\alpha^2 Dt}$$

Space dependent portion

$$\frac{\partial^2 \Phi}{\partial r^2} + \frac{1}{r}\frac{\partial \Phi}{\partial r} + \alpha^2 \Phi(r) = 0$$

$$r^2 \frac{\partial^2 \Phi}{\partial r^2} + r \frac{\partial \Phi}{\partial r} + r^2 \alpha^2 \Phi(r) = 0$$

set $\omega = r\alpha$

$$\omega^2 \frac{\partial^2 \Phi}{\partial \omega^2} + \omega \frac{\partial \Phi}{\partial \omega} + \omega^2 \Phi(\omega) = 0$$

Obtain Eigenmode:

$$\Phi(r\alpha) = AJ_\alpha(r\alpha) + BY_\alpha(r\alpha)$$

General Solution:

$$C(r, t) = \sum_{n=1}^{\infty} (AJ_0(r\alpha_n) + BY_0(r\alpha_n))e^{-\alpha_n^2 Dt}$$

To satisfy boundary conditions, the eigenmode is equivalent to

$$U_0(\alpha r) = J_0(\alpha r)Y(\alpha R_2) - J_0(\alpha R_2)Y_0(\alpha r)$$

because $U_0 = 0$ at $r = R_1$ and $r = R_2$ given that α is a root of the following equation [Carslaw and Jaeger]:

$$J_0(\alpha R_1)Y_0(\alpha R_2) - J_0(\alpha R_2)Y_0(\alpha R_1) = 0 \quad (1)$$

Given orthogonality relationships of Bessel functions of the First and Second kind

$$\int_{R_1}^{R_2} r U_0(\alpha r) U_0(\beta r) dr = 0$$

Where α and β are different roots of (1).

$$\int_{R_1}^{R_2} r U_0^2(\alpha r) dr = \frac{1}{2\alpha^2} \left[\left(r \frac{dU_0}{dr} \right)^2 \right]_{R_1}^{R_2} = \frac{2\{J_0^2(\alpha R_1) - J_0^2(\alpha R_2)\}}{\pi^2 \alpha^2 J_0^2(\alpha R_1)}$$

$$\int_{R_1}^{R_2} r U_0(\alpha r) dr = -\frac{1}{\alpha^2} \left[r \frac{dU_0}{dr} \right]_{R_1}^{R_2} = \frac{2\{J_0(R_1\alpha) - J_0(R_2\alpha)\}}{\pi \alpha^2 J_0(R_1\alpha)}$$

$$\int_{R_1}^{R_2} r U_0(\alpha r) \ln r dr = -\frac{1}{\alpha^2} \left[r \ln r \frac{dU_0}{dr} \right]_{R_1}^{R_2} = \frac{2\{J_0(R_1\alpha) \ln R_2 - J_0(R_2\alpha) \ln R_1\}}{\pi \alpha^2 J_0(R_1\alpha)}$$

Which are found by the following known relationships from Craslow and Jaeger:

$$\left[r \frac{dU_0}{dr} \right]_{r=R_2} = \alpha R_2 [J_0'(\alpha R_2) Y_0(\alpha R_2) - Y_0'(\alpha R_2) J_0(\alpha R_2)] = -\frac{2}{\pi}$$

$$\left[r \frac{dU_0}{dr} \right]_{r=R_1} = \alpha R_1 [J_0'(\alpha R_1) Y_0(\alpha R_2) - Y_0'(\alpha R_1) J_0(\alpha R_2)] = \frac{\alpha R_1}{\rho} [J_0'(\alpha R_1) Y_0(\alpha R_1) - Y_0'(\alpha R_1) J_0(\alpha R_1)] = -\frac{2}{\pi \rho}$$

By defining the following

$$\frac{J_0(R_1\alpha)}{J_0(R_2\alpha)} = \frac{Y_0(R_1\alpha)}{Y_0(R_2\alpha)} = \rho$$

Setting the initial condition as a Fourier Bessel-series expansion,

$$f(r) = A_1 U_0(\alpha_1 r) + A_2 U_0(\alpha_2 r) + \dots$$

Integrating both sides from R_1 to R_2 and multiplying by r and U_0 , assuming each term can be integrated individually, we simplify to get the following:

$$A_n = \frac{\pi^2 \alpha_n^2}{2} \frac{J_0^2(R_1 \alpha_n)}{J_0^2(R_1 \alpha_n) - J_0^2(R_2 \alpha_n)} \int_{R_1}^{R_2} r f(r) U_0(r \alpha_n) dr$$

Plugging in A_n into the homogeneous boundary conditions of the general solution, we obtain:

$$C_{homogenous} = \frac{\pi^2}{2} \sum_{n=1}^{\infty} \frac{\alpha_n^2 J_0^2(R_1 \alpha_n)}{J_0^2(R_1 \alpha_n) - J_0^2(R_2 \alpha_n)} e^{-D \alpha_n^2 t} U_0(r \alpha_n) \int_{R_1}^{R_2} r f(r) U_0(r \alpha_n) dr$$

Putting back the steady-state solution (insert back the "poison tooth")

$$C(r, t) = C_{ss} + C_{homogeneous}$$

where

$$C_{ss} = \frac{C(r = R_1) \ln\left(\frac{R_2}{r}\right) + C(r = R_2) \ln\left(\frac{r}{R_1}\right)}{\ln\left(\frac{R_2}{R_1}\right)}$$

$$\begin{aligned} C(r, t) = & \frac{\pi^2}{2} \sum_{n=1}^{\infty} \frac{\alpha_n^2 J_0^2(R_1 \alpha_n)}{J_0^2(R_1 \alpha_n) - J_0^2(R_2 \alpha_n)} e^{-D \alpha_n^2 t} U_0(r \alpha_n) \int_{R_1}^{R_2} r f(r) U_0(r \alpha_n) dr \\ & - \pi \sum_{n=1}^{\infty} \frac{\{C(r = R_2) J_0(R_1 \alpha_n) - C(r = R_1) J_0(R_2 \alpha_n)\} J_0(R_1 \alpha_n) U_0(r \alpha_n)}{J_0^2(R_1 \alpha_n) - J_0^2(R_2 \alpha_n)} e^{-D \alpha_n^2 t} \\ & + \frac{C(r = R_1) \ln\left(\frac{R_2}{r}\right) + C(r = R_2) \ln\left(\frac{r}{R_1}\right)}{\ln\left(\frac{R_2}{R_1}\right)} \end{aligned}$$

where $C_0 = 0, C(r = R_1) = 0$, we arrive at the final solution:

$$C(r, t) = -\pi \sum_{n=1}^{\infty} \frac{C(r = R_2) J_0(R_1 \alpha_n) J_0(R_1 \alpha_n) U_0(r \alpha_n)}{J_0^2(R_1 \alpha_n) - J_0^2(R_2 \alpha_n)} e^{-D \alpha_n^2 t} + \frac{C(r = R_2) \ln\left(\frac{r}{R_1}\right)}{\ln\left(\frac{R_2}{R_1}\right)}$$

Appendix B – Matlab and Mathematica Code

```
function project
%%% BENG 221 Matthew Cai A08195697

clear;
close all

%%% Project

global C0 D R1 R2 T Km Vm v
C0 = 0; %mM
D = 1.23*10^-9; %mm^2/s %1.23*10^-9; %m^2/s
R1 = 0.0001;%m (100 um)
R2 = 0.00085;%m (850 um)
T = 140; %sec
Km = 4; %mM
Vm = 0.5; %mM/s
v = -0.00017; %m/s

% solution using finite differences
dx=(R2-R1)/100;
dt=1/50;
xmesh=R1:dx:R2;
tmesh=0:dt:T;
[x,t]=meshgrid(xmesh,tmesh);
nx = length(xmesh); % number of points in x dimension
nt = length(tmesh); % number of points in t dimension
stepsize = D * dt / dx^2; % stepsize for numerical integration
sol_fd = zeros(nt, nx);
sol_fd(:,1)=sol_fd(:,1); %BC at R1 is value 0
sol_fd(:,nx)=sol_fd(:,nx)+20; %BC at R2 is value 20

%sol_fd(1, :) = (c0/2)*(1-cos(2*pi*xmesh/L)); % initial conditions;

for t = 2:nt
    for x = 2:nx-1
        %Numerical solution with Convection and Consumption
        %
        sol_fd(t,x) = sol_fd(t-1,x) + stepsize * ...
            (sol_fd(t-1,x+1) - 2 * sol_fd(t-1, x) + sol_fd(t-1,x-1)) +
        ...
        %
        stepsize/(2*x)*(sol_fd(t-1,x+1)-sol_fd(t-1,x-1)) - ...
        %
        v*dt/(2*dx)*(sol_fd(t-1,x+1)-sol_fd(t-1,x-1)) - ...
        %
        Vm*dt*sol_fd(t-1,x)/(Km+sol_fd(t-1,x));

        %Numerical solution without convection
        sol_fd(t,x) = sol_fd(t-1,x) + stepsize * ...
            (sol_fd(t-1,x+1) - 2 * sol_fd(t-1, x) + sol_fd(t-1,x-1)) +
        ...
            stepsize/(2*x)*(sol_fd(t-1,x+1)-sol_fd(t-1,x-1)) - ...
            Vm*dt*sol_fd(t-1,x)/(Km+sol_fd(t-1,x));

        %Numerical Solution without convection or consumption
        %
        sol_fd(t,x) = sol_fd(t-1,x) + stepsize * ...
            (sol_fd(t-1,x+1) - 2 * sol_fd(t-1, x) + sol_fd(t-1,x-1)) +
        ...
```

```

%             stepsize/(2*x)*(sol_fd(t-1,x+1)-sol_fd(t-1,x-1));
    end
end

figure
surf(xmesh,tmesh,sol_fd, 'EdgeColor', 'none')
title('Finite differences')
xlabel('r [m]')
ylabel('t [sec]')
zlabel('c(r,t) [mM]')

c=xmesh;
for n=1:length(xmesh)
    c(n)=20*log(xmesh(n)/0.0001)/log(0.00085/0.0001);
end

fd_fun = sol_fd(nt,:);

figure
plot(xmesh,fd_fun,'*',xmesh,c,'+')
title('Concentration Profile of Steady State Solutions')
legend('Numerical soln with consumption and convection','Analytical soln
without consumption and convection')
xlabel('x [m]')
ylabel('c(x) [mM]')

[x,t]=meshgrid(xmesh,tmesh);

figure
f = analyticaltext(x,t);
surf(x,t,f,'EdgeColor','none')
title('Analytical Solution: No consumption or convection (8 roots)')
axis([R1 R2 0 T 0 20])
xlabel('x [m]')
ylabel('t [sec]')
zlabel('conc [mM]')

function [f] = analyticaltext(x,t)
global C0 D R1 R2

roots = [0.39993 0.82486 1.24694 1.66779 2.08799 2.50781 2.9274 3.34683];
%found from FindRoots in Mathematica with R1=1 and R2=8.5
roots = 10000*roots; %convert for R1=0.0001 and R2=0.00085

f=20.*log(x/R1)./log(R2/R1);
for n=1:1:8
    f = f + ...
        (-(pi*20*besselj(0,R1*roots(n))^2/(besselj(0,R1*roots(n))^2-
besselj(0,R2*roots(n))^2)) ...
        *(besselj(0,x.*roots(n))*bessely(0,R2*roots(n))-
besselj(0,R2*roots(n)).*bessely(0,x.*roots(n))).* exp(-D.*roots(n)^2.*t);
%     f = f + ...
%
    ((pi*C0*besselj(0,R1*roots(n))/(besselj(0,R1*roots(n))+besselj(0,R2*roots(n))
))...

```

```

%      -(pi*20*besselj(0,R1*roots(n))^2/(besselj(0,R1*roots(n))^2-
besselj(0,R2*roots(n))^2))...
%      *(besselj(0,x.*roots(n))*bessely(0,R2*roots(n))-
besselj(0,R2*roots(n)).*bessely(0,x.*roots(n))).* exp(-D.*roots(n)^2.*t);

```

end

Mathematica:

```

a=1;
b=8.5;
N[FindRoot[BesselJ[0,a*x]*Bessely[0,b*x]-
BesselJ[0,b*x]*Bessely[0,a*x],{x,3.3}],10]

```